

ACCURATE SIMULATION OF DELAMINATION GROWTH UNDER MIXED-MODE LOADING USING COHESIVE ELEMENTS WITH MODE-DEPENDENT PENALTY STIFFNESS

A.Turon^{*,1}, E.V. González^{*}, P. Maimí^{*}, P. Camanho[†], J. Costa^{*}

^{*}AMADE, University of Girona
Campus Montilivi, s/n. 17071 Girona, Spain

Albert.turon@udg.edu
Emilio.gonzalez@udg.edu
Pere.maimi@udg.edu
Josep.costa@udg.edu

[†]DEMec, Universidade do Porto
Rua Dr. Roberto Frias 4200-465 Porto, Portugal
pcamanho@fe.up.pt

ABSTRACT

The cohesive zone model approach, in conjunction with a damage formulation has been used by many authors to simulate delamination using finite element codes. Most of these models available in the literature are developed for pure mode loading, and then extended to analyze mixed-mode loading situations. However, these models have not been validated correctly under mixed-mode loading conditions where an incorrect selection of the parameters of the model can result in inaccurate simulation predictions. To obtain accurate simulation results, the cohesive formulation previously developed by the authors has been modified. Mode-dependent penalty stiffness has been introduced in the formulation as well as the damage evolution law has been redefined. Different loading scenarios are simulated to validate the accuracy of the new formulation presented.

KEY WORDS: Delamination, mixed-mode, cohesive zone model.

1. INTRODUCTION

Delamination is one of the most common types of damage in laminated fiber-reinforced composites due to their relatively weak interlaminar strengths. Delamination or interlaminar damage may arise under mode I loading and under mode II loading, however in practical applications, delamination is more likely to grow under mixed-mode loading conditions. An effective method to analyze delamination is using cohesive zone models [1-5].

Cohesive zone models provide an ideal representation of the delamination process of advanced composite materials. The excellent performance of cohesive zone models in the simulation of delamination is due to the accurate kinematics representation of the fracture process, based on a strong discontinuity in the displacement field and to the possibility to use constitutive models that correctly account for the different loading modes.

The cohesive zone model approach, in conjunction with a damage formulation has been used by many authors to simulate delamination using finite element codes. Moreover, the latest versions of commercial nonlinear

finite element codes incorporate the capability to simulate delamination. Most of these models available in the literature are developed for pure mode loading, mode I or mode II loading, and then extended to analyze mixed-mode loading situations. However, these models have not been validated correctly under mixed-mode loading conditions where an incorrect selection of the material properties can result in inaccurate simulation results [6]. To obtain accurate simulation results, a reformulation of the cohesive formulation developed by the authors [3,5] is presented in this paper. The formulation is modified by introducing mode-dependent penalty stiffness and redefining the damage evolution law. Different mixed-mode loading scenarios are simulated to validate the accuracy of the formulation presented.

2. REFORMULATION OF THE COHESIVE DAMAGE MODEL

The constitutive behaviour of cohesive elements is implemented using a cohesive damage zone model that relates the tractions, τ , to the displacement jumps, Δ , at the interfaces where crack propagation occurs. Damage

¹ Corresponding author

initiation is related to the interfacial strength of the material, τ^0 . When the energy dissipated is equal to the Fracture Toughness of the material, G_c , the traction is reduced to zero and new crack surfaces are formed. The constitutive law used in this work is a bilinear relation between the tractions and the displacement jumps [5,7]. The bilinear cohesive law uses an initial linear elastic response before damage initiation, as shown in Figure 1. This linear elastic part is defined using a penalty stiffness parameter, K , that ensures a stiff connection between the surfaces before crack propagation. The interfacial strength and the penalty stiffness define an onset displacement jump, Δ^0 , related to the initiation of damage.

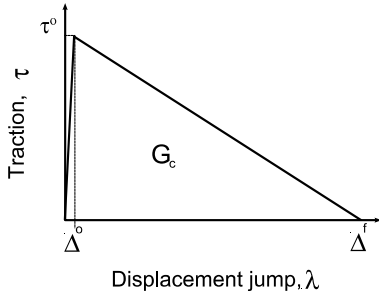


Figure 1 Bilinear constitutive law used for quasi-static loading.

The displacement jump across the interface is obtained from the displacements of the points located on the top and bottom sides of the interface in the local coordinate system.

Further detail of the boundary value problem and the kinematics of the model are detailed in [3,5]. In the following sections the reformulation of the constitutive equations is described.

2.1 Constitutive equations

The Helmholtz free energy by unit surface of the interface under isothermal conditions is divided in two terms:

$$\Psi(\Delta, d) = \Psi(\Delta, d)_{coh} + \Psi(\Delta)_{con} \quad (1)$$

where $\Psi(\Delta, d)_{coh}$ and $\Psi(\Delta)_{con}$ refer to the cohesive and contact energy contributions, respectively. The vector $\Delta = \{\Delta_1, \Delta_2, \Delta_3\}^T$ contains the displacement jumps between the two homologous points of the respective adjacent surfaces, and d is the scalar isotropic damage variable. It should be noted that Δ acts as the free variable (i.e. displacement driven formulation) and d is the internal variable that ensures the irreversibility of the model [5,10].

The definition of the energy terms should be selected such as it yields to a unilateral and a symmetric constitutive behaviour for propagation mode I and shear modes, respectively. The corresponding expressions are:

$$\Psi(\Delta, d)_{coh} = \frac{1}{2}(1-d)[\Delta_i K_{ij} \Delta_j + \Delta_3 \delta_{i3} K_{33} \langle -\Delta_3 \rangle] \quad (1)$$

$$\Psi(\Delta, d)_{con} = -\frac{1}{2} \Delta_3 \delta_{i3} K_{33} \langle -\Delta_3 \rangle \quad (1)$$

where $\langle x \rangle$ are the Macaulay brackets defined as $\langle x \rangle = \frac{1}{2}(x + |x|)$, and δ_{ij} is the Kronecker delta. K_{ij} are the components of the stiffness matrix.

The stiffness matrix is defined as a diagonal matrix, therefore only the diagonal terms: K_{11} , K_{22} and K_{33} are non zero. K_{11} , K_{22} and K_{33} are the penalty stiffness for modes II, III and I, respectively. Applying Coleman's method [2], the constitutive equation reads:

$$\tau_i = \tau_{i,coh} + \tau_{i,con} \quad (2)$$

where

$$\tau_{i,coh} = (1-d)[K_{ij} \Delta_j + \delta_{i3} K_{33} \langle -\Delta_3 \rangle] \quad (3)$$

$$\tau_{i,con} = -\delta_{i3} K_{33} \langle -\Delta_3 \rangle \quad (4)$$

2.1 Equivalent mixed mode norms

To formulate the damage evolution law, a mixed-mode norms of the tractions, τ , and the displacement jumps, λ , have been to be defined. In the original model [3,5] they were defined as the Euclidean norm of the individual tractions and displacement jumps, respectively. However, in the reformulation of the model using different penalty stiffness, these mixed-mode norms need to be redefined. The relation between the mixed-mode traction τ and the mixed-mode displacement jump λ is defined as:

$$\tau = (1-d)k_B \lambda \quad (5)$$

where k_B is a mode-dependent interfacial stiffness.

The mixed-mode traction τ is defined as the Euclidean norm of the individual tractions τ_1 , τ_2 , τ_3 . The mixed-mode displacement jump λ reads:

$$\lambda = \frac{K_{ii} [\Delta_i^2 - \delta_{3i} \langle -\Delta_3 \rangle^2]}{\sqrt{K_{ii} [\Delta_i^2 - \delta_{3i} \langle -\Delta_3 \rangle^2]}} \quad (6)$$

and the mixed-mode interfacial stiffness k_B is defined as:

$$k_B = \frac{K_{ii}^2 [\Delta_i^2 - \delta_{3i} \langle -\Delta_3 \rangle^2]}{K_{ii} [\Delta_i^2 - \delta_{3i} \langle -\Delta_3 \rangle^2]} \quad (7)$$

To completely define the evolution of the damage variable under mixed-mode loading, a local mixed-mode ratio B is defined as:

$$B = \frac{\Psi_1 + \Psi_2}{\Psi} = \frac{K_{11}\Delta_1^2 + K_{22}\Delta_2^2}{K_{11}\Delta_1^2 + K_{22}\Delta_2^2 + K_{33}\langle -\Delta_3 \rangle^2} \quad (8)$$

Defining $K_{sh}=K_{11}=K_{22}$ and using equation (8) in equation (7), the mixed-mode interfacial stiffness results in a condensed form as:

$$k_B = K_{33}(1-B) + BK_{sh} \quad (9)$$

2.3 Damage activation function and evolution law

The damage activation function is defined as:

$$F(\mathbf{\Lambda}) = H(\mathbf{\Lambda}) - r_d \leq 0 \quad (10)$$

where $H(\mathbf{\Lambda})$ is a monotonic loading function which depends on the jump displacement vector, and r_d is the threshold function. Both functions are updated at every time t , and they are respectively defined as:

$$H(\mathbf{\Lambda}) = \min \left\{ \frac{\lambda - \Delta^o}{\Delta^f - \Delta^o}, 1 \right\} \quad (11)$$

$$r_d = \max \left\{ 0, \max_s [H(\mathbf{\Lambda})] \right\} \quad 0 \leq s \leq t \quad \forall t \quad (12)$$

It should be noted that the first term of equation (11) is directly the ratio of the energy dissipated during the damage process and of the critical energy release rate, i.e. G_d/G_c [6]. Therefore, from equations (11) and (12) the expression which defines the damage variable d reads:

$$d = \frac{r_d \Delta^f}{r_d \Delta^f + (1-r_d) \Delta^o} \quad (13)$$

To complete define the constitutive model it is necessary to define the displacement jumps corresponding to delamination onset, Δ^o , and to delamination propagation, Δ^f , under mixed-mode conditions. The Benzeggagh and Kenane criterion [8] is used to define these parameters, yielding to [5]:

$$\Delta^o = \left(\frac{K_{33}(\Delta_3^o)^2 + [K_{sh}(\Delta_{sh}^o)^2 - K_{33}(\Delta_3^o)^2]B^\eta}{k_B} \right)^{\frac{1}{2}} \quad (14)$$

$$\Delta^f = \frac{1}{k_B \Delta^o} (K_{33}\Delta_3^o \Delta_3^f + [K_{33}\Delta_{sh}^o \Delta_{sh}^f - K_{33}\Delta_3^o \Delta_3^f]B^\eta) \quad (15)$$

where Δ_{sh}^o and Δ_3^o are the displacement jumps corresponding to delamination onset in pure mode I and shear mode respectively, and Δ_{sh}^f and Δ_3^f are the displacement jumps corresponding to delamination propagation in pure mode I and shear mode respectively [5].

2.4 Rate of energy dissipation

To ensure the thermodynamic consistency of the model, the dissipated energy by surface unit during the damage propagation process, Ξ , has to be equal or greater than zero:

$$\Xi = Y \dot{d} \geq 0 \quad (16)$$

where the thermodynamic force Y associated with the internal variable d is defined as:

$$Y = \frac{1}{2} d [\Delta_i K_{ij} \Delta_j + \Delta_3 \delta_{i3} K_{33} \langle -\Delta_3 \rangle] \quad (17)$$

Equation (17) demonstrates that the thermodynamic force Y is always equal or greater than zero; therefore the term \dot{d} must be positive. Since the damage variable is a function of r_d and the local mixed-mode ratio B , the following equation must be satisfied:

$$\dot{d} = \frac{\partial d}{\partial r_d} \dot{r}_d + \frac{\partial d}{\partial B} \dot{B} \geq 0 \quad (18)$$

The threshold function r_d is always positive according to equation (12), and the term $\frac{\partial d}{\partial r_d}$ is also always positive:

$$\frac{\partial d}{\partial r_d} = \frac{\Delta^o \Delta^f}{[r_d \Delta^f + (1-r_d) \Delta^o]^2} \quad (19)$$

Therefore, since the local mixed-mode ratio B can either increase or decrease, the term $\frac{\partial d}{\partial B}$ must be zero to ensure the thermodynamic consistency of the model:

$$\frac{\partial d}{\partial B} = \frac{\partial \frac{\Delta^o}{\Delta^f}}{\partial B} \quad (20)$$

Previous equation is equivalent to the condition given in [6] for the selection of the pure mode interfacial stiffness. Using the initiation and propagation criteria given in previous section, the condition to ensure the thermodynamic consistency reads:

$$K_{sh} = K_{33} \frac{G_{Ic}}{G_{IIc}} \left(\frac{\tau_{shear}^o}{\tau_3^o} \right)^2 \quad (21)$$

3. VALIDATION EXAMPLES

Simulations of delamination propagation under pure mode I, pure mode II, and mixed-mode loading are performed. The double cantilever beam (DCB) and the end-notched flexure (ENF) test specimens are used to simulate delamination propagation under pure mode I and under pure mode II loading respectively. The mixed-mode bending (MMB) test specimen is used to simulate delamination growth under mixed-mode loading. The configurations of the DCB, ENF and MMB test specimens are shown in Figure 1.

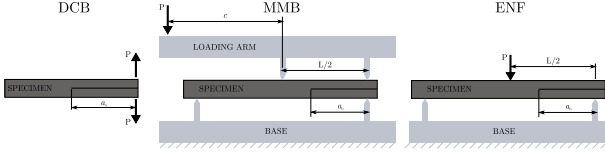


Figure 2. DCB, MMB, and ENF test specimens.

Four-node cohesive elements implemented as Abaqus user elements [3,5] and two-dimensional plane stress elements (Abaqus CPE4 elements) are used to simulate DCB, MMB, and ENF tests in unidirectional carbon-fiber reinforced epoxy composite. The specimens simulated are 150mm long, 20mm wide, with two 1.55mm thick arms, with an initial crack length of 3 mm. A mode I penalty stiffness of $K_{33}=10^6 \text{N/mm}^3$ is used. The remaining material properties are $E_{11}=120 \text{GPa}$, $E_{22}=E_{33}=10.5 \text{GPa}$, $G_{12}=G_{13}=5.25 \text{MPa}$, $G_{23}=3.48 \text{MPa}$, $\nu_{12}=\nu_{13}=0.3$, $\nu_{23}=0.5$, $G_{Ic}=0.260 \text{kJ/m}^2$ and $G_{IIc}=1.002 \text{kJ/m}^2$.

Models using 0.15mm long cohesive elements along the length of the specimen, and 10 plane stress elements along the specimen's thickness are created to simulate the DCB, MMB and ENF tests with the different interface strengths τ_3^o and τ_{sh}^o . The initial size of the delamination in the DCB and MMB specimens is simulated by removing the corresponding cohesive elements. For the ENF specimen, pre-damaged cohesive elements are placed in the pre-cracked region to avoid interpenetration of the crack faces.

Several simulations with the same elastic and fracture properties but with different values of τ_3^o using the DCB test specimen are performed. The results are compared with the analytical expressions obtained using LEFM which depend only on the fracture toughness. The relation between the applied load and the displacement is shown in Figure 3 where it can be observed that the results during crack propagation match the LEFM solution, regardless of the interface strength. Lower values of the interlaminar strength result in lower values of the maximum applied load. Nevertheless, there are no differences in the load-displacement curve when steady state delamination growth takes place.

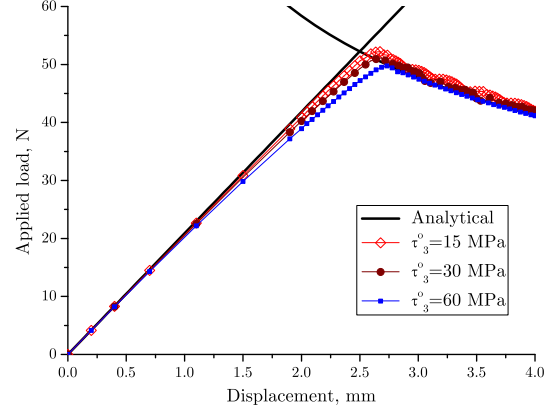


Figure 3. Load displacement curve obtained for different interface strengths in a DCB test.

Similar simulations are performed to predict delamination growth under pure mode II loading for different values of τ_{sh}^o using the ENF test specimen. The relation between the applied load and the displacement is shown in Figure 4. As observed in the pure mode I tests, the results obtained match the LEFM curve during self-similar delamination growth, regardless of the interface strength.

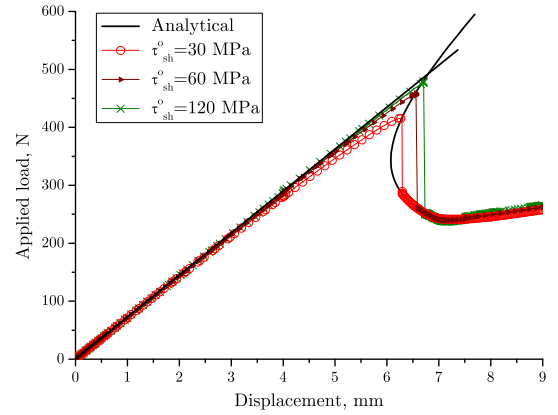


Figure 4. Load displacement curve obtained for different interface shear strengths in a ENF test.

A similar exercise is performed for specimens under mixed-mode loading. A mixed-mode ratio of 50% is simulated by setting the distance c shown in Figure 1 to 63.18mm [9]. Several simulations with the same elastic and fracture properties but with different interface strengths are performed. The interface strengths are varied to investigate their effect on the results. The results obtained are presented in Figure 4, where it can be observed that the load-displacement relation during crack propagation is independent on the strength used.

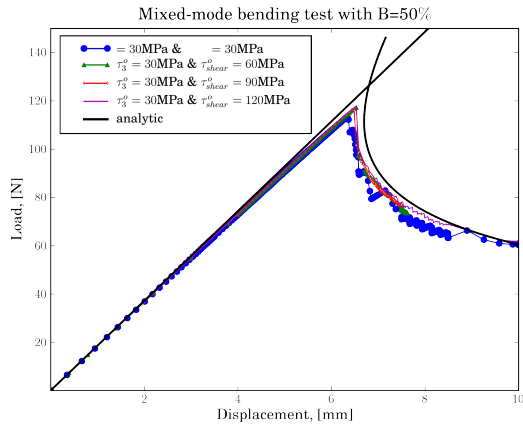


Figure 5. Load displacement curve obtained for different interface strengths in a MMB test with 50% of mode II.

From Figure 5 is also observed that the computed energy dissipation during delamination grow is independent of the interlaminar shear strength.

4. CONCLUSIONS

The cohesive element formulation previously developed by the authors has been reformulated to get accurate predictions under mixed-mode loading. The formulation has been modified by introducing mode-dependent penalty stiffness and redefining the activation function, the damage evolution law, and the equivalent mixed-mode norms of the displacement jump. It has demonstrated that exist a relation between the pure mode interface stiffness and the cohesive properties (pure mode Fracture Toughness and pure mode interface strengths). The accuracy of the new model has been demonstrated by simulating delamination under different mixed-mode loading conditions. It has shown that the computed energy dissipation under delamination propagation is independent of the interface strengths selected.

ACKNOWLEDGEMENTS

The authors would like to acknowledge the useful discussions with Dr. Carlos G. Dávila, NASA Langley Research Center, U.S.A.

This work has been partially funded by the Spanish government through DG- GICYT under contract: MAT2006-14159-C02-01 and the research visit of the first author at the University of Porto funded by the grant JC2008-00400 of the José Castillejos" program. The financial support of the Portuguese Foundation for Science and Technology (FCT) under the project PTDC-EME-PME-64984-2006 is acknowledged.

REFERENCES

- [1] G. Alfano, M. Crisfield, Finite element interface models for the delamination analysis of laminated composites: mechanical and computational issues, *International Journal for Numerical Methods in Engineering*, 77 (2) (2001), 111-170.
- [2] U. Mi, M. Crisfield, G. Davies, Progressive delamination using interface elements, *Journal of Composite Materials*, 32 (1999), 1246-1272.
- [3] P.P. Camanho, C.G. Dávila, M. de Moura, Numerical simulation of mixed-mode progressive delamination in composite materials, *Journal of Composite Materials*, 37 (2003), 1415-1438.
- [4] V. Goyal-Singhal, E. Johnson, C.G. Dávila, Irreversible constitutive law for modeling the delamination process using interfacial surface discontinuities, *Composite Structures*, 64 (2004), 91-105.
- [5] A. Turon, P.P. Camanho, J. Costa, C.G. Dávila, "A damage model for the simulation of delamination in advanced composites under variable-mode loading", *Mechanics of Materials*, 38:1079-1089, 2006.
- [6] A. Turon, P.P. Camanho, J. Costa, J. Renart, Accurate simulation of delamination growth under mixed-mode loading using cohesive elements: definition of interlaminar strengths and elastic stiffness, *Journal of composite materials*, (2009), submitted.
- [7] E. Reddy Jr., F. Mello, T. Guess, Modeling the initiation and growth of delaminations in composite structures, *Journal of Composite Materials*, 31 (1997), 812-831.
- [8] M.L. Benzeggagh, M. Kenane, Measurement of Mixed-Mode delamination Fracture Toughness of Unidirectional Glass/Epoxy Composites With Mixed- Mode Bending Apparatus, *Composites Science and Technology*, 49 (1996), 439-49.
- [9] N. Blanco, A. Turon, J. Costa, An exact solution for the determination of the mode mixture in the mixed-mode bending delamination test, *Composites Science and Technology* 66 (10), (2006), 1256-1258.
- [10] E.V. González, P. Maimí, A. Turon, P.P. Camanho and J. Renart, Simulation of delamination by means of cohesive elements using an explicit finite element code, *CMC - Computers, Materials and Continua*, 9, 51-92, (2009).